Inorg. Chem. **2007**, *46*, 3459–3466

Inorganic Chemistry
Article

New Methacrylate-Functionalized Ba and Ba–Ti Oxoclusters as Potential Nanosized Building Blocks for Inorganic–Organic Hybrid Materials: Synthesis and Characterization

Alberto Albinati,[†] Francesco Faccini,[‡] Silvia Gross,*[,‡] Guido Kickelbick,[§] Silvia Rizzato,[†] and Alfonso Venzo[‡]

Dipartimento di Chimica Strutturale e Stereochimica Inorganica, Universitá degli Studi di Milano, Via Venezian, 21, Milan, Italy, Istituto di Scienze e Tecnologie Molecolari, ISTM-CNR, Dipartimento di Scienze Chimiche, Universitá degli Studi di Padova, via Marzolo, 1, Padova, Italy, INSTM, and Institut für Materialchemie, TU Wien, Getreidemarkt 9/165-1040 Vienna, Austria

Received August 17, 2006

Two different methacrylate modified barium–titanium and barium-based oxoclusters, $Ba_2Ti_{10}(\mu_3\text{-}O)_8(\mu_2\text{-}OH)_5(\mu_2\text{-}OMc)_{20}(O^iPrOMe)_2$ (**1**) and $[Ba(OMc)_2(McOH)_3]_n$ (**2**), were synthesized by reacting methacrylic acid with barium–titanium and barium–zirconium double alkoxides, respectively. The X-ray structure determination of oxocluster **1** shows a core consisting of a ring of 10 titania octahedra, sharing corners, that surround the two barium oxygen decaeders which are linked by common edges to the titania octahedra and the neighboring barium decaeder. The solid-state structure of **2** consists of zigzag chains of edge-sharing $\{BaO_9\}$ polyhedra linked through bridging bidentate metacrylate anions, displaying different coordination mode of carboxylate groups. The presence of methacrylate groups surrounding the two polynuclear compounds has been exploited for the embedding of the oxocluster in inorganic–organic hybrid materials, and some preliminary results are presented.

Introduction

Materials with new and enhanced properties can be obtained by combining, at a molecular level, inorganic and organic building blocks. This class of materials, known as inorganic–organic hybrid materials, is currently an intensively explored topic of research. A wide plethora of inorganic–organic hybrid materials has been described extensively in recent papers and reviews.[1–13] Major focus is devoted to inorganic–organic hybrids in which the components are linked through covalent or ionic strong chemical bonds. In this framework, a primary concern in the development of inorganic–organic hybrid materials is the design and the synthesis of suitable inorganic building blocks which can be embedded into the polymeric matrix by the formation of covalent bonds, e.g., via copolymerization. Among these precursors, suitably functionalized metal oxoclusters, polyoxometalates, and polynuclear metal complexes and compounds have received much attention because they afford versatility in both composition and structure of the oxoclusters. In this regard, the choice of suitable functional groups such as polymerizable moieties can ensure an easy covalent incorporation of the inorganic unit into the polymer backbone. Different organically modified transition-

---

[*] To whom correspondence should be addressed. E-mail: silvia.gross@unipd.it.

[†] Universitá degli Studi di Milano.

[‡] Universitá degli Studi di Padova and INSTM.

[§] TU Wien.

(1) Sanchez, C.; Julian, B.; Belleville, P.; Popall, M. *J. Mater. Chem.* **2005**, *15*, 3559 and references therein.
(2) Special Issue on Organic-Inorganic Nanocomposite. *Chem. Mater.* **2001**, *13*.
(3) Sanchez, C.; Soler-Illia, G. J. d. A. A.; Ribot, F.; Lalot, T.; Mayer, C. R.; Cabuil, V. *Chem. Mater.* **2001**, *13*, 3061.
(4) Sanchez, C.; Ribot, F.; Lebeau, B. *J. Mater. Chem.* **1999**, *9*, 35.
(5) Sanchez, C.; Romero-Gomez, P. *Hybrid Functional Materials*; Wiley-VCH: 2004.
(6) Wen, J.; Wilkes, G. L. *Chem. Mater.* **1996**, *8*, 1667.
(7) Sharp, K. G. *Adv. Mater.* **1998**, *10*, 1243.
(8) Loy, D. A. *MRS Bull.* **2001**, *May*, 364.
(9) Spanhel, L.; Popall, M.; Müller, G. *Proc. - Indian Acad. Sci., Chem. Sci.* **1995**, *107*, 637.
(10) Schubert, U. *Chem. Mater.* **2001**, *13*, 3487 and references therein.
(11) Kickelbick, G. *Prog. Polym. Sci.* **2003**, *28*, 83 and references therein.
(12) Schubert, U. *J. Sol–Gel Sci. Technol.* **2003**, *26*, 47 and references therein.
(13) Schubert, U. Polymers Reinforced by Covalently-Bonded Metal Oxide Clusters. In *Organic/Inorganic Hybrid Materials*, Electronic Publ. Services: Hattiesburg, MI, 2003; and references therein.

10.1021/ic0615630 CCC: $37.00

metal oxoclusters have been synthesized by Schubert and co-workers[10,12,13] and by other groups. Furthermore polynuclear compounds characterized by different metals, shapes, and nuclearity were prepared and throughly characterized, based on different transition metals such as Y,[14,15] Ti,[16−18] Zr,[19−25] Ta,[26] and Hf.[21] Other mixed oxoclusers were synthesized and structurally characterized based on Ti−Y,[27] Zr−Ti,[28] Ti−Hf−Zr,[21] and Hf−Ti.[21] To the best of our knowledge, no barium-based oxoclusters functionalized with polymerizable groups have been reported yet. Kessler et al. have prepared different mixed Ba−Zr[29] and Ba−Ti[30,31] species functionalized with saturated alkyl groups. Hubert-Pfalzgraf and co-workers have reported the synthesis of mixed polynuclear Ba−Ce[32] and Ba−Bi[33] and other Ba-based[34] species, while the synthesis of several bimetallic alkoxides has been addressed with the aim of developing mixed oxide materials.[35−39] Polynuclear barium β-diketonate derivatives with amino alcohols have also been structurally characterized.[40] Briceno et al.[41] have synthesized a two-dimensional barium mesaconate tetrahydrate polymeric oxocluster. Further barium-based polyoxometalates have been synthesized and described in the literature.[42−44] Few studies have been reported on Ba−Ti hybrid materials. $BaTiO_3$-based hybrid materials have been prepared starting from barium and methacrylate-modified titanium alkoxides.[45,46] In a study by Tang et al.,[47] the preparation and characterization of $BaTiO_3$ superfine fibers-based IPN is described.

Table 1. Crystal Data and Structure Refinement Parameters for **1** and **2**

compound	**1**	**2**
empirical formula	$C_{88}H_{118}Ba_2O_{57}Ti_{10}$	$C_{20}H_{28}Ba_2O_{10}$
M_w	2841.50	565.75
data coll T, K	173	200
λ [Å]	0.71073	0.71073
crystal system	monoclinic	monoclinic
space group	$P2_1/n$ (14)	Cc (9)
a, Å	14.4641(5)	14.567(5)
b, Å	31.169(1)	26.263(5)
c, Å	31.012(1)	7.251(5)
β, deg	92.991(1)	115.935(5)
V, Å^3	13961.9(8)	2495(2)
Z	4	4
$\rho_{(calcd)}$ g cm^{-3}	1.352	1.506
$F(000)$	5736	1136
μ (mm^{-1})	1.170	1.639
no. data collected	64562	8225
no. independent data	16972	3801
no. obs reflns (no) $[\lvert F_o\rvert^2 > 2.0\sigma(\lvert F\rvert^2)]$	9435	3358
R_{int}[a]	0.0876	0.0875
R_1[a]	0.0726	0.0877
R_1 (obs reflns)[a]	0.0493	0.0768
wR_2 (obs reflns)[a]	0.1202	0.1573
GOF[a]	1.020	1.140

[a] $R_{int} = \sum|F_o^2 - F_o^2(\text{mean})|/\sum[F_o^2]$, $R_1 = \sum||F_o| - |(1/k)F_c||/\sum|F_o|$, $wR_2 = [\sum w(F_o^2 - (1/k)F_c^2)^2/\sum w|F_o^2|^2]^{1/2}$, $\text{GOF} = [\sum w(F_o^2 - (1/k)F_c^2)^2/(n_o - n_v)]^{1/2}$.

In this work, we have prepared two different barium- and barium−titanium polynuclear species functionalized with methacrylate groups which could be used to covalentely anchor the oxocluster to an acrylate monomer and to embed the oxocluster into a polymer backbone.

Experimental Section

General Comments. All reaction and manipulations were carried out under an argon atmosphere by using standard Schlenk or septum/cannula techniques. $BaTi(OR)_6$ and $BaZr(OR)_6$, purchased by ABCR GmbH, Karlsruhe, Germany, were used as received while methacrylic acid 99.5% (purchased by Aldrich, Milan, Italy) was distilled in reduced pressure before use. All reactants were stored under argon atmosphere. Methylmethacrylate (MMA) and dibenzoylperoxide (BPO) were purchased by Aldrich, Milan, Italy. Anhydrous KBr was purchased by Merck GmbH, Germany,

Elemental analyses were obtained in the Microanalysis Laboratory of the Department of Chemistry of the University of Padova by using a Frisons EA 1108 instrument.

---

(14) Fric, H.; Jupa, M.; Schubert, U. *Monatsh. Chem.* **2006**, *137*, 1−6.

(15) Hubert-Pfalzgraf, L. G.; Daniele, S. *C. R. Chim.* **2004**, *7*, 521−527.

(16) Schubert, U. *J. Mater. Chem.* **2005**, *15*, 3701−3715.

(17) Mijatovic, I.; Kickelbick, G.; Puchberger, M.; Schubert, U. *New J. Chem.* **2003**, *27*, 3−5.

(18) Mijatovic, I.; Kickelbick, G.; Schubert, U. *Eur. J. Inorg. Chem.* **2001**, *8*, 1933−1935.

(19) Kickelbick, G.; Wiede, P.; Schubert, U. *Inorg. Chim. Acta* **1999**, *284*, 1−7.

(20) Trimmel, G.; Gross, S.; Kickelbick, G.; Schubert, U. *Appl. Organomet. Chem.* **2001**, *15*, 410.

(21) Gross, S.; Kickelbick, G.; Puchberger, M.; Schubert, U. *Monatsh. Chem.* **2003**, *134*, 1053.

(22) Moraru, B.; Kickelbick, G.; Battistella, M.; Schubert, U. *J. Organomet. Chem.* **2001**, *636*, 172−174.

(23) Moraru, B.; Gross, S.; Kickelbick, G.; Trimmel, G.; Schubert, U. *Monatsh. Chem.* **2003**, *132*, 993−999.

(24) Kickelbick, G.; Feth, M. P.; Bertagnolli, H.; Puchberger, M.; Holzinger, D.; Gross, S. *J. Chem. Soc., Dalton Trans.* **2002**, *20*, 3892−3898.

(25) Puchberger, M.; Kogler, F. R.; Jupa, M.; Gross, S.; Fric, H.; Kickelbick, G.; Schubert, U. *Eur. J. Inorg. Chem.* **2006**, *16*, 3283−3293.

(26) Gross, S.; Di Noto, V.; Kickelbick, G.; Schubert, U. *Mater. Res. Soc. Symp. Proc.* **2002**, *726*, Q4.1.1−Q4.1.9.

(27) Jupa, M.; Kickelbick, G.; Schubert, U. *Eur. J. Inorg. Chem.* **2004**, *9*, 1835 −1839.

(28) Moraru, B.; Kickelbick, G.; Schubert, U. *Eur. J. Inorg. Chem.* **2001**, *5*, 1295−1301.

(29) Seisenbaeva, G. A.; Gohil, S.; Kessler, V. G. *J. Mater. Chem.* **2004**, *14*, 3177−3190.

(30) Kessler, V. G.; Hubert-Pfalzgraz, L. G.; Daniele, S.; Gleizes, A. *Chem. Mater.* **1994**, *6*, 2336−2342.

(31) Yanovsky, A. I.; Yanovskaya, M. I.; Limar, V. K.; Kessler, V. G.; Turova, N. Y.; Struchkov, Y. T. *J. Chem. Soc., Chem. Commun.* **1991**, *122*, 1605.

(32) Hubert-Pfalzgraf, L. G.; Sirio, C.; Bois, C. *Polyhedron* **1998**, *17*, 821−830.

(33) Parola, S.; Papiernik, R.; Hubert-Pfalzgraf, Bois, C. *J. Chem. Soc., Dalton Trans.* **1998**, *5*, 737−739.

(34) Hubert-Pfalzgraf, L. G. *Phosphorous, Sulfur Silicon Relat. Elem.* **2001**, *168*, 69−76.

(35) Daniele, S.; Hubert-Pfalzgraf, L. G.; Vaissermann, J. *Polyhedron* **1998**, *17*, 4249−4256.

(36) Hubert-Pfalzgraf, L. G.; Guillon, H. *Appl. Organomet. Chem.* **1998**, *12*, 4249−4256.

(37) Hubert-Pfalzgraf, L. G. *J. Coord. Chem. Rev.* **1998**, *178−180*, 967−998.

(38) Hubert-Pfalzgraf, L. G. *J. Mater. Chem.* **2004**, *14*, 3113−3123.

(39) Hubert-Pfalzgraf, L. G. *Chem. Rev.* **1990**, *90*, 969−995.

(40) Hubert-Pfalzgraf, L. G.; Labrize, F.; Bois, C. *Polyhedron* **1994**, *13*, 2163−2172.

(41) Briceno, A.; Delgado, J. M.; Diaz del Delgado, G. *Acta. Crystallogr., Sect. E: Struct. Rep. Online* **2002**, *E58*, m602−m605.

(42) Qin, C.; Wang, X. L.; Qi, Y. F.; Wang, E. B.; Hu, C. W.; Xu, L. J. *Solid State Chem.* **2004**, *177*, 3263−3269.

(43) Wang, J. P.; Duan, X. Y.; Niu, J. Y. *J. Mol. Struct.* **2004**, *693*, 187−191.

(44) Zhang, Y. P.; Haushalter, R. C.; Zubieta, J. *Inorg. Chim. Acta* **1998**, *277*, 263−267.

(45) Weiner, H.; Lunk, H. J.; Ziemer, B.; Kohnke, K.; Pietzsch, C. *Thermochim. Acta* **1994**, *244*, 93−103.

(46) Yogo, T.; Yamamoto, T.; Sakamoto, W.; Hirano, S. *J. Mater. Res.* **2004**, *19*, 3290−3297.

(47) Tang, D. Y.; Qiang, L. S.; Jin, Z.; Cai, W. M. *J. Appl. Polym. Sci.* **2002**, *84*, 709−715.

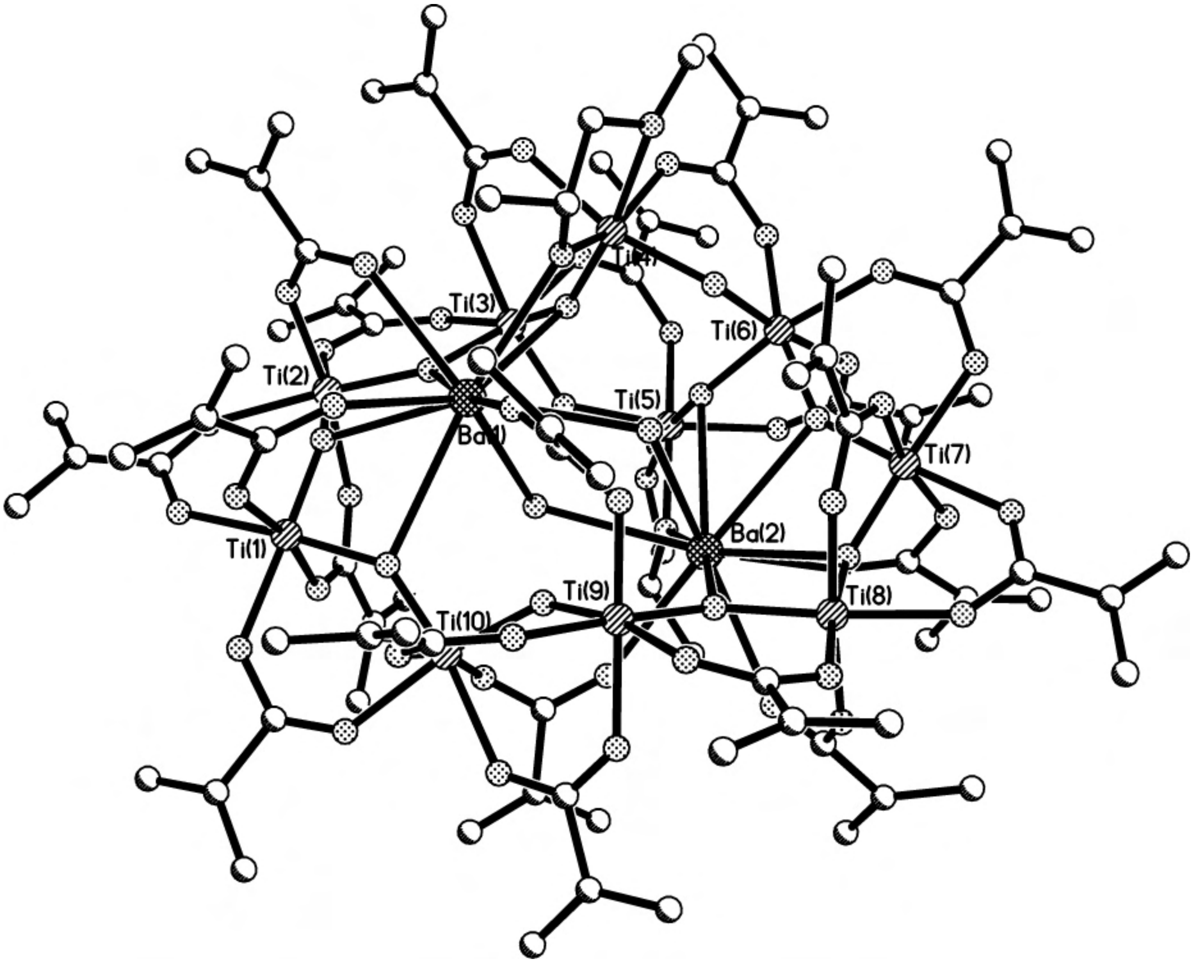

Figure 1. Molecular structure of the oxocluster $Ba_2Ti_{10}(\mu_3\text{-}O)_8(\mu_2\text{-}OH)_5(\mu_2\text{-}OMc)_{20}(O^iPrOMe)_2$.

NMR Experimental Section. ^1H and ^{13}C NMR spectra were obtained at different temperatures as acetone-d_6 solutions on a Bruker DRX-400 spectrometer operating at 400.13 and 100.61 MHz, respectively, and equipped with a BVT2000 temperature controller. The chemical shift values are given in δ units with reference to internal Me_4Si. Suitable integral values for the proton spectra were obtained by a prescan delay of 10 s. The assignments of the proton resonances were performed by standard chemical shift correlations and 2D *CO*rrelation *S*pectroscop*Y* (COSY), *TO*tal *C*orrelation *S*pectroscop*Y* (TOCSY), and *N*uclear *O*verhauser *E*nhancement Spectroscop*Y* (NOESY) experiments. The ^{13}C resonances were attributed through 2D-heterocorrelated COSY experiments (*H*eteronuclear *M*ultiple *Q*uantum *C*orrelation, HMQC) with *Bi*linear *R*otation-*D*ecoupling, BIRD, sequence[48] and HMBC[49] and quadrature along F1 achieved using the *T*ime-*P*roportional receiver *P*hase *I*ncrementation, TPPI, method[50,51]for the H-bonded carbon atoms and *H*eteronuclear *M*ultiple *B*ond *C*orrelation, HMBC[49] for the quaternary ones.

FT−IR Study. FT−IR experiments were performed with a NEXUS 870 FT−IR (NICOLET), operating in the transmission range 400−4000 cm^{-1}, collecting 32 scans with a spectral resolution of 4 cm^{-1}. The measurements were recorded by dispersing the oxocluster in anhydrous KBr.

Crystallography. Crystals suitable for X-ray diffraction were mounted on a Bruker SMART diffractometer, equipped with a CCD detector, and cooled, using a cold nitrogen stream, to 173 K for **1** and 200 K for **2**, respectively.

The space groups were determined from the systematic absences, while the cell constants were refined, at the end of the data collection with the data reduction software SAINT.[52] Data were collected by using ω-scans in the range $2° < \theta_{max} < 27°$ for **1** and $2° < \theta_{max} < 25°$ for **2**. Experimental conditions and crystallographic and other relevant data are listed in Table 1 and in the Supporting Information.

The intensities were corrected for Lorentz and polarization factors[52] and empirically for absorption using the SADABS program.[53]

The structures were solved by direct methods (SHELXS97)[54] and refined by full-matrix least-squares on F^2 (SHELXL97) using anisotropic displacement parameters for all non-hydrogen atoms. Hydrogen atoms, in calculated positions, were refined using a riding model ($B(H) = 1.2 \times B(C_{bonded})(Å^2)$).

The scattering factors used, corrected for the real and imaginary parts of the anomalous dispersion, were taken from the literature.[55] All calculations were carried out by using the PC version of the

---

(48) Bax, A.; Subramian, S. *J. Magn. Reson*. **1986**, *67*, 565.
(49) Bax, A.; Summers, M. F. *J. Am. Chem. Soc*. **1986**, *108*, 2093.
(50) Otting, G.; Wüthrich, K. *J. Magn. Reson*. **1988**, *76*, 569.
(51) Drobny, G.; Pines, A.; Sinton, S.; Weitekamp, D.; Wemmer, D. *Faraday Symp. Chem. Soc.* **1979**, *B33*, 4912.
(52) *BrukerAXS, SAINT, Integration Software*; Bruker Analytical X-ray Systems: Madison, WI, 1995.
(53) Sheldrick, G. M. *SADABS, Program for Absorption Correction*; University of Göttingen: Göttingen, Germany, 1996.
(54) Sheldrick, G. M. *SHELX-97. Structure Solution and Refinement Package*; Universität Göttingen: 1997.

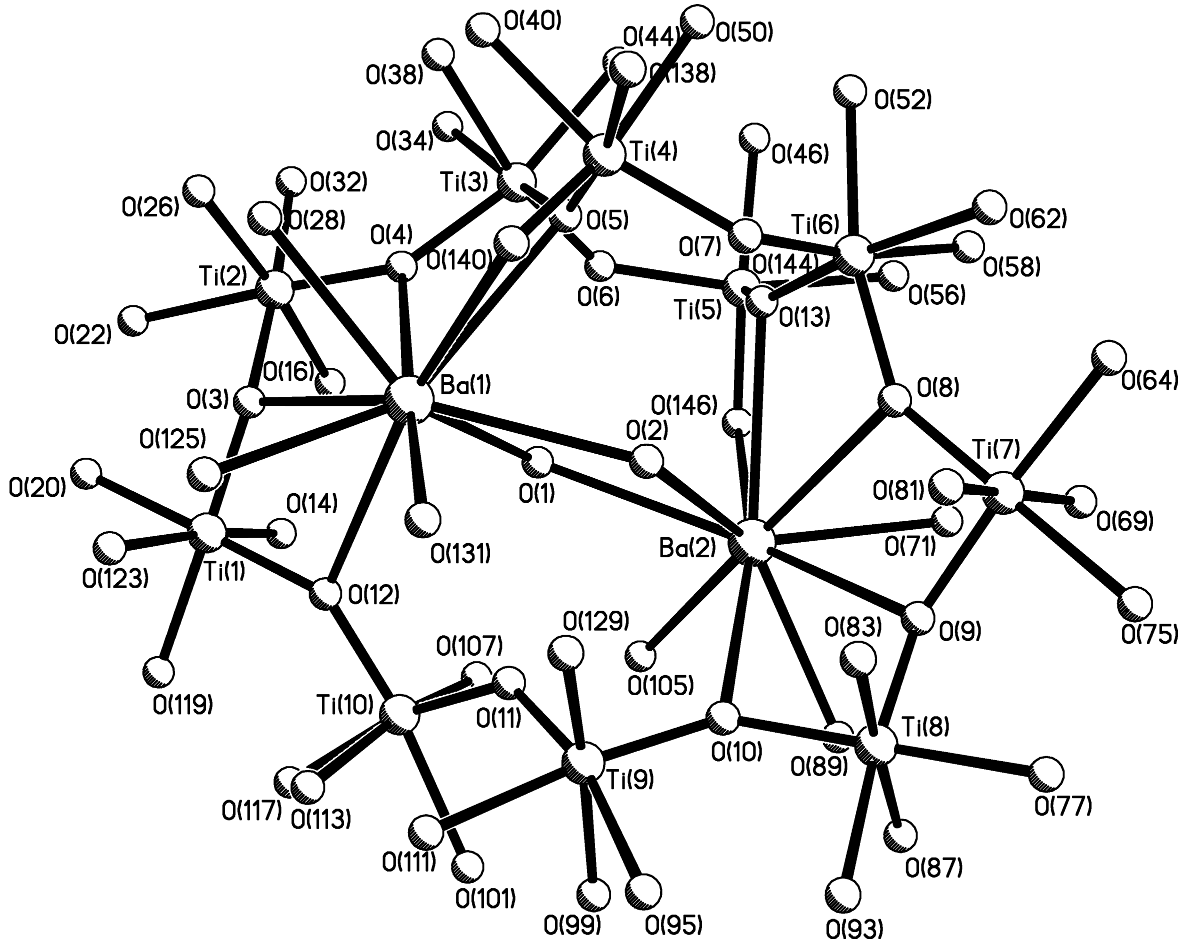

Figure 2. Structure of the metal oxo core of oxocluster **1**.

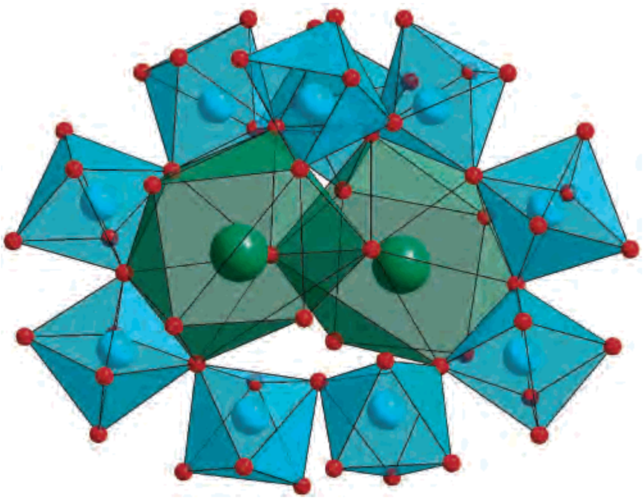

Figure 3. The metal oxo core of oxocluster **1** in polyhedral representation.

following programs: WINGX,[56] SHELX-97,[54] ORTEP,[57] and DIAMOND.[58] The *R* values for the structures are relatively high due to the bad quality of the crystals and to the presence of large cavities in the crystal packing which contain disordered solvent molecules. However, refinements of these structures by applying suitable models for the disorder did not significantly decrease the *R* values.

NMR Data of BaTi(O^{i}PrOMe)$_6$ Solution. ^{1}**H NMR** (δ, $CDCl_3$, 298 K): 3.66 (m, $H_3CC\mathbf{H}(O^-)CH_2OCH_3$), 3.10 (s, $H_3CCH(O^-)CH_2OC\mathbf{H_3}$), 3.05 (m, $H_3CCH(O^-)C\mathbf{H}^AH^BOCH_3$), 2.99 (m, $H_3CCH(O^-)CH^A\mathbf{H}^BOCH_3$), 0.88 (t, $\mathbf{H_3}CCH(O^-)CH_2OCH_3$). ^{13}**C{**^{1}**H} NMR** (δ, $CDCl_3$, 298 K): 18.6 ($H_3\mathbf{C}CH(O^-)CH_2OCH_3$), 65.7 ($H_3C\mathbf{C}H(O^-)CH_2OCH_3$), 78.2 ($H_3CCH(O^-)\mathbf{C}H_2OCH_3$), 58.6 ($H_3CCH(O^-)CH_2O\mathbf{C}H_3$).

Synthesis of $\mathbf{Ba_2Ti_{10}(\mu_3\text{-}O)_8(\mu_2\text{-}OH)_5(\mu_2\text{-}OMc)_{20}(O^iPrOMe)_2}$ (1). To 1.12 g of a 0.5 M solution of BaTi(O^{i}PrOMe)$_6$ (0.55 mmol) was added dropwise 1.12 g (13.0 mmol) of methacrylic acid, thus obtaining a alkoxide/carboxylic acid molar ratio of 1/24. The reaction mixture was then allowed to stand at room temperature for 25 days, resulting in the separation of brown crystals soluble in toluene and THF. The crystals were separated by the mother liquors by decanting and then dried in vacuum for 12 h at room temperature. Yield: 2.32 g (0.54 mmol, 91%). Elem. Anal. Calculated for $C_{88}H_{118}Ba_2O_{57}Ti_{10}$. Found (Calc.) C: 39.95 (37.16); H: 6.02 (4.15).

The obtained higher values in the elemental analysis can be ascribed to the presence of residual solvent molecules remaining entrapped in the oxocluster structure. In fact, the experimental values are higher than those expected on the basis of the oxocluster formula.

NMR Data of $\mathbf{Ba_2Ti_{10}(\mu_3\text{-}O)_8(\mu_2\text{-}OH)_5(\mu_2\text{-}OMc)_{20}(O^iPrOMe)_2}$. ^{1}**H NMR** ($\delta$, $CDCl_3$, 298 K): 6.14 (s, $\mathbf{H}^{cis}HC{=}C(CH_3)COO^-$), 5.61 (s, $\mathbf{H}^{trans}HC{=}C(CH_3)COO^-$)), 1.87 (s, $H_2C{=}C(C\mathbf{H_3})COO^-$.

---

[55] *International Tables for X-ray Crystallography*; Wilson, A. J. C., Ed.; Kluwer Academic Publisher: Dordrecht, The Netherlands, 1992; Vol. C.

[56] Farrugia, L. J. *J. Appl. Crystallogr.* **1999**, *32*, 837.

[57] Farrugia, L. J. *J. Appl. Crystallogr.* **1997**, *30*, 565.

[58] Brandenburg, K. *DIAMOND. Version 3.0;* Crystal Impact GbR: Bonn, Germany, 1996−1998.

Table 2. Selected Bond Distances (Å) for Compound **1**

Ba(1)−O(125)	2.740(1)	Ti(6)−O(52)	2.059(7)
Ba(1)−O(131)	2.747(8)	Ti(6)−O(62)	2.065(10)
Ba(1)−O(3)	2.783(7)	Ti(6)−O(58)	2.094(9)
Ba(1)−O(28)	2.791(9)	Ti(7)−O(8)	1.785(7)
Ba(1)−O(140)	2.815(7)	Ti(7)−O(9)	1.850(7)
Ba(1)−O(1)	2.851(7)	Ti(7)−O(69)	1.966(10)
Ba(1)−O(4)	2.960(7)	Ti(7)−O(81)	2.015(10)
Ba(1)−O(12)	3.006(6)	Ti(7)−O(64)	2.065(9)
Ba(1)−O(2)	3.020(7)	Ti(7)−O(75)	2.117(8)
Ba(1)−O(5)	3.084(6)	Ti(7)−Ti(8)	3.366(3)
Ba(1)−Ti(2)	3.753(2)	Ti(8)−O(9)	1.784(7)
Ba(1)−Ti(1)	3.768(2)	Ti(8)−O(10)	1.869(8)
Ba(2)−O(105)	2.734(10)	Ti(8)−O(87)	1.906(9)
Ba(2)−O(71)	2.760(12)	Ti(8)−O(93)	2.046(8)
Ba(2)−O(9)	2.780(7)	Ti(8)−O(77)	2.048(10)
Ba(2)−O(89)	2.797(10)	Ti(8)−O(83)	2.063(9)
Ba(2)−O(2)	2.829(7)	Ti(9)−O(10)	1.788(8)
Ba(2)−O(146)	2.835(7)	Ti(9)−O(11)	1.822(7)
Ba(2)−O(8)	2.898(7)	Ti(9)−O(129)	1.932(7)
Ba(2)−O(1)	2.985(8)	Ti(4)−O(140)	1.857(7)
Ba(2)−O(10)	3.023(7)	Ti(4)−O(7)	1.931(7)
Ba(2)−O(13)	3.062(6)	Ti(4)−O(50)	2.010(8)
Ba(2)−Ti(7)	3.721(2)	Ti(4)−O(40)	2.073(9)
Ba(2)−Ti(8)	3.792(2)	Ti(4)−O(138)	2.279(9)
Ti(1)−O(3)	1.784(7)	Ti(4)−Ti(6)	3.387(3)
Ti(1)−O(12)	1.856(7)	Ti(5)−O(13)	1.730(7)
Ti(1)−O(123)	1.906(10)	Ti(5)−O(146)	1.863(7)
Ti(1)−O(119)	2.029(9)	Ti(5)−O(6)	1.905(8)
Ti(1)−O(14)	2.046(9)	Ti(5)−O(46)	2.033(7)
Ti(1)−O(20)	2.060(10)	Ti(5)−O(56)	2.053(10)
Ti(1)−Ti(2)	3.363(3)	Ti(5)−O(144)	2.259(9)
Ti(2)−O(4)	1.775(8)	Ti(6)−O(7)	1.778(7)
Ti(2)−O(3)	1.848(7)	Ti(6)−O(8)	1.850(6)
Ti(2)−O(26)	1.913(10)	Ti(6)−O(13)	1.916(7)
Ti(2)−O(32)	2.032(9)	Ti(9)−O(99)	2.023(8)
Ti(2)−O(16)	2.056(10)	Ti(9)−O(111)	2.089(9)
Ti(2)−O(22)	2.129(10)	Ti(9)−O(95)	2.094(8)
Ti(3)−O(6)	1.775(7)	Ti(9)−Ti(10)	3.365(3)
Ti(3)−O(4)	1.857(7)	Ti(10)−O(12)	1.786(7)
Ti(3)−O(5)	1.913(7)	Ti(10)−O(11)	1.835(7)
Ti(3)−O(34)	2.058(9)	Ti(10)−O(107)	1.948(9)
Ti(3)−O(44)	2.072(8)	Ti(10)−O(113)	2.008(8)
Ti(3)−O(38)	2.083(9)	Ti(10)−O(117)	2.081(9)
Ti(3)−Ti(5)	3.380(3)	Ti(10)−O(101)	2.129(8)
Ti(4)−O(5)	1.740(7)		

Additional signals (ca. 5%, by integration): 3.85 (m, $H_3CC\mathbf{H}(O^-)CH_2OCH_3$), 3.30 (s, $H_3CCH(O^-)CH_2OC\mathbf{H_3}$), 3.09 (m, $H_3CCH(O^-)C\mathbf{H_2}OCH_3$), 1.04 (t, $\mathbf{H_3}CCH(O^-)CH_2OCH_3$). **^{13}C NMR** ($\delta$, $CDCl_3$, 298 K): 173.4 ($H_2C{=}C(-CH_3)\text{-}\mathbf{C}OO^-$), 136.2 ($H_2\mathbf{C}{=}C(-CH_3)\text{-}COO^-$), 127.5 ($H_2C{=}\mathbf{C}(-CH_3)\text{-}COO^-$), 17.9 ($H_2C{=}C(\text{-}\mathbf{C}H_3)\text{-}COO^-$).

FT−IR Data of $Ba_2Ti_{10}(\mu_3\text{-}O)_8(\mu_2\text{-}OH)_5(\mu_2\text{-}OMc)_{20}(O^iPrOMe)_2$. 3338 (w br), 3022 (w, νCH), 2881 (m, νCH), 2846 (w br, $\nu O{-}CH_3$), 2825 (w, $\nu O\text{-}CH_2$), 2767 (w br), 2485 (w br), 1869 (w), 1687 (s, $\nu C{=}O$), 1697 (s, $\nu C{=}O$), 1637 (s, $\nu C{=}C$), 1603 (m, $\nu C{-}O^-_{\text{alkoxide}}$), 1535 (s, $\nu_{as}COO^-$), 1456 (s, $\delta_{as}CH_3$), 1411 (s, ν_sCOO^-), 1371 (s, δ_sCH_3), 1323 (m), 1300 (m), 1261 (w), 1245 (m), 1217 (m, γCH_3), 1201 (s, γCH_3), 1178 (m, $\nu_sC{-}O_{\text{ester}}$), 1095 (w, $\nu_{as}C{-}O_{\text{ester}}$), 1009 (m), 935 (s, $\delta_{\text{out of plane}}C{=}C$), 852 (w), 821 (w), 802 (m), 703 (w br), 657 (w, νTi−O−Ti), 613 (m, νTi−O), 603 (m, νTi−O) 590 (m, νTi−O), 542 (w), 435 (w, νTi−O−Ti) cm^{-1}.

Synthesis of $[Ba(OMc)_2(McOH)_3]_n$ (2). 1.68 g (0.55 mmol) of a 0.33 M solution of $BaZr(O^iPrOMeR)_6$ in *n*-butanol was mixed with 1.64 g (19 mmol) of methacrylic acid, thus obtaining an alkoxide/carboxylic acid molar ratio of 1:35. The reaction mixture was then allowed to stand at room temperature for 25 days, resulting in the separation of colorless crystals soluble in toluene and THF. The crystals were separated by the mother liquors by decanting and then dried in vacuum for 12 h at room temperature.

NMR Data of $[Ba(OMc)_2(McOH)_3]_n$. ^{1}H NMR (δ, $CDCl_3$, 298 K): 6.21 and 6.01 (two m, $\mathbf{H}^{cis}HC{=}C(-CH_3)\text{-}COO^-$), 5.64 and 5.32 (two m, $\mathbf{H}^{trans}HC{=}C(-CH_3)\text{-}COO^-$), 1.93 and 1.79 (two s, $H_2C{=}C(-C\mathbf{H_3})\text{-}COO^-$). The two sets integrate in the ratio 9:1, respectively. Additional signals (ca. 10%, by integration): 3.95 (m, $H_3CC\mathbf{H}(O^-)CH_2OCH_3$), 3.45 (s, $H_3CCH(O^-)CH_2OC\mathbf{H_3}$), 3.21 (m, $H_3CCH(O^-)C\mathbf{H_2}OCH_3$) 1.04 (t, $C\mathbf{H_3}CH(O^-)CH_2OCH_3$).

FT−IR Data of $[Ba(OMc)_2(McOH)_3]_n$. 3101 (w, νCH), 2960 (w, νCH), 2927 (w, νCH), 2858 (w br), 2684 (w br), 2570 (w br), 2491 (w br), 1869 (m), 1697 (s, $\nu C{=}O$), 1687 (s, $\nu C{=}O$), 1637 (s, $\nu C{=}C$), 1574 (s, $\nu_{as}COO^-$), 1535 (s, $\nu_{as}COO^-$), 1456 (s, δCH_3), 1423 (s, ν_sCOO^-), 1371 (s, δ -CH_3), 1323 (m), 1300 (m), 1261 (m), 1245 (m), 1217 (m, γCH_3), 1201 (s, γCH_3), 1178 (m, $\nu_sC{-}O_{\text{ester}}$), 1095 (m, $\nu_{as}C{-}O_{\text{ester}}$), 1009 (m), 935 (s, $\delta_{\text{out of plane}}(C{=}C)$), 883 (w), 852 (m), 821 (m), 802 (s), 660 (m), 617 (m), 590 (m), 542 (m), 503 (m), 467 (m), 422 (m), 400 (m) cm^{-1}.

Synthesis of the Inorganic−Organic Hybrid Materials. To a weighed amount of $Ba_2Ti_{10}(\mu_3\text{-}O)_8(\mu_2\text{-}OH)_5(\mu_2\text{-}OMc)_{20}(O^iPrOMe)_2$, **(1)**, dissolved in toluene, was added MMA to achieve **1**:MMA molar ratios of 50, 100, and 200. To this solution was added the thermoinitiator BPO (3% w/w with respect to the monomer), and the solution was stirred and heated to 60 °C for 6 h. After removal of the solvent by heating at 70 °C in vacuum for 12 h, glassy, transparent materials were obtained.

Results and Discussion

Description of the Structures. The $Ba_2Ti_{10}(\mu_3\text{-}O)_8(\mu_2\text{-}OH)_5(\mu_2\text{-}OMc)_{20}(O^iPrOMe)_2$ (**1**) oxocluster consists of two BaO_{10} cores moieties surrounded by 10 TiO_6 octahedra. The resulting "oxocluster core" is surrounded by a shell of 10 methacrylate groups acting as bridging ligands between titanium atoms (Figure 1−3).

In addition two 3-methoxy-2-propanolate ligands are coordinated to the oxocluster (of which one is disordered with two equivalent positions (C97, C98A/B, C99A/B, C10A/B)). Eight μ_3-O (O13, O45, O64, O77, O114, O127, O140, O142) and five μ_2-OH (O32, O141, O143, O144, O145) groups act as bridging atoms between the metals (Figure 2). The μ_2-OH groups (O142, O143) form the edges shared by the two BaO_{10} polyhedrons. In both polyhedra long Ba−O separations (Ba1−O143: 299.3(3) pm, Ba1−O144: 282.9(3) pm, Ba2−O143: 281.9(3) pm, Ba2−O144: 300.3(3) pm) are present and form unsymmetrical bridges to the two bonded Ba-atoms. All the TiO_6 octahedra are connected by corner-shared oxygen atoms forming a sort of helical environment around the BaO_{10} polyhedra. Four TiO_6 polyhedra display edge-sharing contacts to one of the two BaO_{10} octahedra. Selected distances are listed in Table 2, and details of the structure analysis are shown in Table 1.

The building blocks of compound **2** can be represented as $[Ba(OMc)_2(McOH)_3]_n$ and consists of *zigzag* chains built by edge-sharing $\{BaO_9\}$ polyhedra running along the [0 0 1] direction. The chains are linked through bridging bidentate methacrylate anions (Figures 4−6). The contacts between adjacent Ba···Ba in the chains are ca. 4.4 Å.

The divalent barium ions are coordinated by nine oxygen atoms at distances in the range 2.8−2.9 Å, from eight carboxylate groups, displaying different coordination modes. The resulting coordination geometry around the Ba atom,

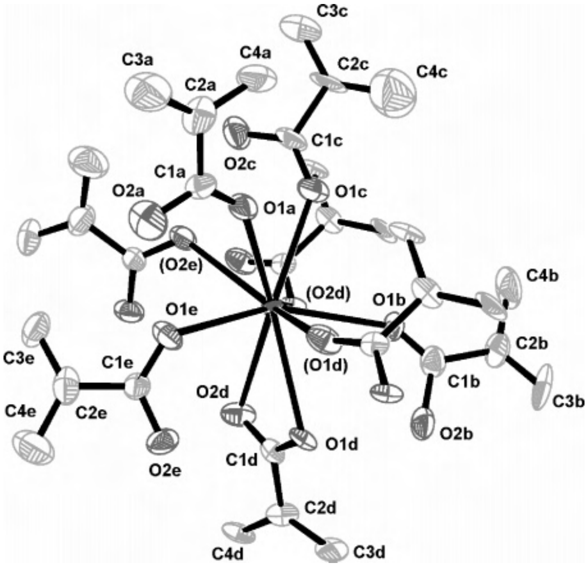

Figure 4. Ortep-III view of the coordination of methacrylic acid molecules and metacrylate ions around Ba^{2+} ion in **2**. Displacement ellipsoids are drawn at the 50% probability level. Hydrogen atoms are omitted for clarity.

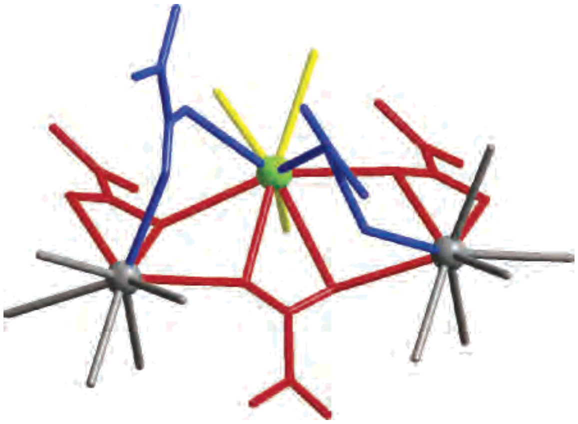

Figure 5. Fragment of polymer showing the different coordination modes of the ligand in **2**.

shown in Figure 4, may be described as a distorted rectangular monocapped antiprism.

The asymmetric unit contains five independent ligand molecules, three in the protonated acid form and two in the anionic form, as confirmed by the C···O bond distances (see Table 3). The former acts as monodentate groups, whereas the latter function as bridging ligands generating the polymer chains.

In particular, the O1E-C1E-O2E carboxylate (colored in blue in Figure 5) adopts a *syn*−*syn* $\mu-\eta^2$ coordination fashion to bridge adjacent metal centers, while O1D-C1D-O2D (colored in red in Figure 5) displays a combination of symmetrical chelating and monoatomic *anti*−*anti* bridging modes, allowing the coordination to three different Ba atoms.

A similar Ba coordination has been found in polymeric species based on mesaconic acid as ligand. To the best of our knowledge, this compound is one of the only two metal salts of α,β-unsaturated carboxylic acids structurally characterized.[41,59]

The 1D polymers in **2** span the same direction but on alternating planes stacking perpendicular to the crystallographic *b*-axis at with an interlayer distance of 11.26 Å equal to $^1/_2$**b**. The packing reveals also that there are not relevant interactions between the polymer chains.

NMR Analysis. In the ^{1}H NMR spectrum of **1**, broad signals at δ 6.14, δ 5.61, and δ 1.87 due to the olefin and methyl protons of the methacrylate can be observed. The position and the line width of these resonances do not change significantly on lowering the temperature from 298 to 228 K, indicating that, in these experimental conditions, no dynamic exchange of the methacrylate between the non-equivalent position found in the solid-state groups can be detected. The ^{13}C NMR resonances, which appear at δ 173.4, δ 136.2, δ 127.5, and δ 17.9 for the carbonyl, the C-2, the C-1, and the methyl carbon in the methacrylate moieties, respectively, behave similarly. It is evident that, in solution, the crystalline interactions are mainly released, giving rise to near-equivalent methacrylate moieties. Finally, no signals attributable to OH proton are observable.

Two sets of less-intense NMR signals indicate also the partial (ca. 5%) esterification 2-(1-methoxy)propoxy residues with methacrylic acid, accordingly to the proposed mechanism for the formation of the oxocluster.[23] The ester signals were identified by comparison with the spectra of references samples.

The ^{1}H NMR spectrum of CDCl$_3$ solutions of the **2** compound show two sets of large resonances at (δ 6.21, δ 5.64, δ 1.93) and (δ 6.01, δ 5.32, δ 1.79) due to methacrylic moieties which integrate in the approximate molar ratio of 9:1. A very broad band, centered at δ 8.0, is attributable to the OH protons of methacrylic acid. Even in this case, the position and the line width of the resonances do not change significantly on lowering the temperature up to −80 °C.

Two additional sets of NMR signals indicate the partial (ca. 10%) esterification of some 2-(1-methoxy)propoxy residues with methacrylic acid. The presence of the ester byproduct in both the compounds could justify the results of the elemental analysis, which reveal for **1** a content of both carbon and hydrogen higher than expected. The presence of residual ester could be ascribed to the not complete removal of this byproduct due to to the very mild conditions applied to dry the two crystalline compounds after they were separated by the mother liquors.

FT−IR Analysis. By analyzing the IR spectra of oxocluster **1**, the nature of the interactions between the metals atom and the carboxylate groups could be elucidated. The spectrum, shown in Figure 1SM in the Supporting Information, is characterized by the presence of two bands at 1535 and 1411 cm^{-1} assigned, respectively, to the asymmetric and symmetric stretching of the carboxylate group, in agreement with the bonding mode shown in the X-ray structure.

Moreover, it is worth noticing that a difference between the symmetric and asymmetric stretching vibration (Δ) of about 124 cm^{-1} is ascribable to the bidentate bridging coordination.[60] At 1637 cm^{-1} the band of C═C double bond of the methacrylate groups surrounding the oxocluster can be recognized, while at 940 cm^{-1} the band of the CH out-

---

(59) Allen, F. H.; Kennard, O. *Chem. Des. Autom. News* **1993**, *8*, 1, 31−37.

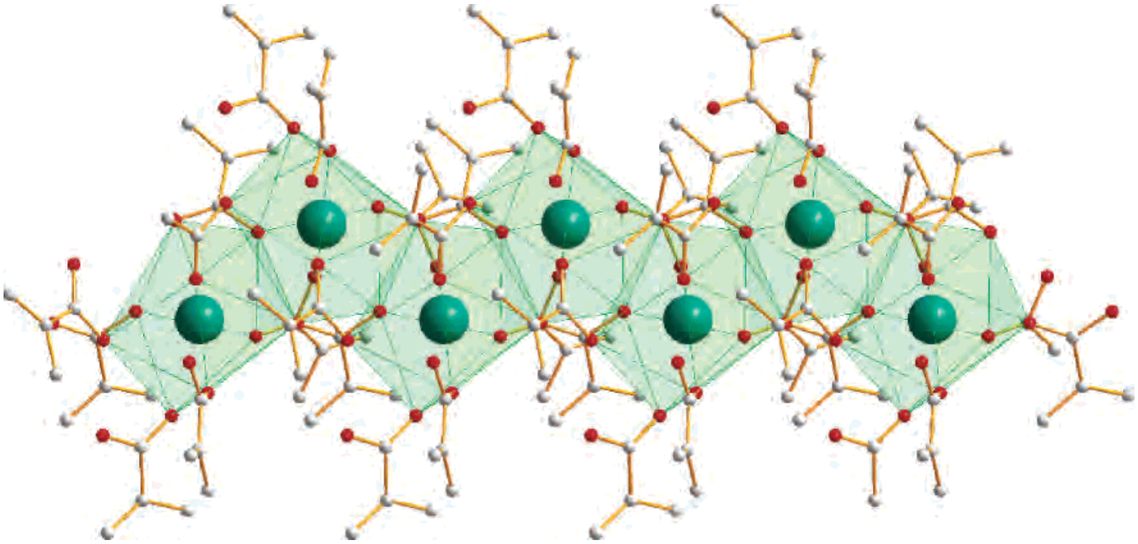

Figure 6. A view down ***a*** of *zigzag* chains of $\{BaO_9\}$ polyhedra in the structure of **2**.

Table 3. Selected Bond Distances (Å) for Compound **2**

Ba−O(1A)	2.816(11)	C(2B)−C(3B)	1.31(3)
Ba−O(1B)	2.780(11)	C(2B)−C(4B)	1.45(3)
Ba−O(1C)	2.778(12)	C(1C)−O(2C)	1.27(2)
Ba−O(1D)	2.871(11)	C(1C)−O(1C)	1.23(2)
Ba−O(1E)	2.784(12)	C(1C)−C(2C)	1.51(2)
Ba−O(1D)#3	2.892(10)	C(2C)−C(3C)	1.37(3)
Ba−O(2D)#1	2.733(11)	C(2C)−C(4C)	1.49(3)
Ba−O(2D)#3	2.836(11)	C(1D)−O(2D)	1.240(18)
Ba-O(2E)#2	2.765(12)	C(1D)−O(1D)	1.289(17)
Ba−Ba#3	4.433(2)	C(1D)−C(2D)	1.52(2)
C(1A)−O(1A)	1.19(2)	C(2D)−C(3D)	1.38(3)
C(1A)−O(2A)	1.31(2)	C(2D)−C(4D)	1.39(2)
C(1A)−C(2A)	1.49(2)	C(1E)−O(1E)	1.232(18)
C(2A)−C(3A)	1.34(3)	C(1E)−O(2E)	1.259(18)
C(2A)−C(4A)	1.45(3)	C(1E)−C(2E)	1.49(2)
C(1B)−O(1B)	1.190(19)	C(2E)−C(3E)	1.35(3)
C(1B)−O(2B)	1.37(2)	C(2E)−C(4E)	1.45(3)
C(1B)−C(2B)	1.46(3)		

of-plane deformation was pointed out. The bands at 1456 and 1371 cm^{-1} are ascribed to the asymmetric and symmetric −CH_3 bending of the methacrylic group, respectively.[61] In the lower wavenumbers region, several absorption bands ascribed to M−O bonds were evidenced and attributed on the basis of literature references.[62,63] In particular, the band at 657 cm^{-1} was ascribed to the stretching vibration of the Ti−O−Ti bond of the Ti-oxo bridges, whereas the bands in the range 590−613 cm^{-1} were ascribed to Ti−O vibrations.

Similar features were observed in the IR spectrum of the polynuclear compound **2** shown in Figure 2SM in the Supporting Information. Also in this case, in the IR spectrum three bands ascribed to carboxylate group could be observed. The two bands at 1574 and 1535 cm^{-1} were assigned to the asymmetric COO^- stretching, while the vibration at the 1423 cm^{-1} band was attributed to the symmetric COO^- vibration.[60] This is in agreement with the X-ray structure, which shows two of the five independent ligand molecules in the anionic form.

A further band at 1637 cm^{-1} is ascribed at the C═C double bond present in methacrylic ligand, while the two vibrations at 1697 and 1687 cm^{-1} are due to C═O vibration of free methacrylic acid in the polymeric barium structure.[61]

Use of the $Ba_2Ti_{10}(\mu_3\text{-O})_8(\mu_2\text{-OH})_5(\mu_2\text{-OMc})_{20}(O^iPrOMe)_2$ (1) for the Development of PMMA-Based Inorganic−Organic Hybrid Materials−Preliminary Experiments. The $Ba_2Ti_{10}(\mu_3\text{-O})_8(\mu_2\text{-OH})_5(\mu_2\text{-OMc})_{20}(O^iPrOMe)_2$ **(1)** oxocluster was used for the preparation of PMMA-based inorganic−organic hybrid materials synthesized by reaction of the oxocluster with MMA by using **1** MMA molar ratios of 50, 100, and 200. The hybrid materials, so obtained, were characterized by solid-state NMR, IR, and TGA-DSC analyses. Compound **1** is effectively embedded in the polymer matrix, and the resulting materials display a good degree of polymerization and a higher thermal decomposition temperature than the undoped PMMA. The characterization of the hybrid is still in progess, and the final results will be described in a forthcoming communication.[64]

Conclusions

By reaction of barium−titanium and barium−zirconium double alkoxides with an excess of methacrylic acid, the two different methacrylate modified barium−titanium and barium-based oxoclusters, $Ba_2Ti_{10}(\mu_3\text{-O})_8(\mu_2\text{-OH})_5(\mu_2\text{-OMc})_{20}(O^i\text{-}PrOMe)_2$ (**1**) and $[Ba(OMc)_2(McOH)_3]_n$ (**2**), were synthesized and stucturally characterized. While the oxocluster **1** is characterized by a core consisting of a ring of 10 titania octahedra, sharing corners, that surround the two barium oxygen decaeders which are linked by common edges to the titania octahedra and the neighboring barium decaeder, the oxocluster **2** is instead characterized by an inusual solid-state structure based on zigzag chains of edge-sharing $\{BaO_9\}$ polyhedra linked through bridging bidentate meth-

---

(60) Nakamoto, K. *Infrared and Raman Spectra of Inorganic & Coordination Compound*, 4th ed.; Wiley-Interscience Edition: New York, 1986.

(61) Silverstein, R. M.; Bassler, G.; Morill, T. C. *Spectrometric Identification of Organic Compound*, 5th ed.; John Wiley & Sons: New York, 1963.

(62) Bezrodna, T.; Puchkovska, G.; Shymanovska, V.; Baran, J.; Ratajczak, H. *J. Mol. Struct.* **2004**, *700*, 175−181.

(63) Hwang, U. Y.; Park, H. S.; Koo, K. K. *Ind. Eng. Chem. Res.* **2004**, *43*, 728−734.

(64) Faccini, F; Gross, S.; Müller, K. Manuscript in preparation.

acrylate anions. The two oxoclusters were further characterized by NMR and FT−IR spectroscopy.

The common feature of the two oxoclusters, i.e., the presence of methacrylate groups surrounding the inorganic polyhedra cores, would allow their use as inorganic building blocks for the development of (meth)acrylate-based inorganic−organic hybrid materials. As a matter of fact, the oxocluster **1** has already been incorporated into a PMMA-based polymer network by reacting it with MMA monomers. The preliminary results show an effective embedding of the oxocluster in the polymer matrix and a slight improvement in the thermal properties with respect to the pristine polymer.

Acknowledgment. Prof. Giuliano Bandoli and Prof. Eugenio Tondello, University of Padova, is acknowledged for helpful discussions. The University of Padua, Italy, the Italian INSTM, and the National Research Council (CNR) are acknowledged for financial support. Italian Rectors Conference (CRUI), Ministero degli Affari Esteri, Rome, Italy, Österreichischer Austauschdienst (ÖAD), Vienna, Austria, and Deutscher Akademischer Austauschdienst (DAAD), Bonn, Germany are gratefully acknowledged for the funding of the researchers mobility in the framework of Italy−Germany and Italy−Austria bilateral programs. S. Gross gratefully thanks the DAAD, Bonn, Germany, also for the awarding of a DAAD grant (Stipendium) to finance a research period in Germany.

Supporting Information Available: IR spectra of compounds **1** and **2**, text, and a table of crystallographic data (also as a CIF file). This material is available free of charge via the Internet at http://pubs.acs.org.

IC0615630